THE JOURNAL OF PHYSICAL CHEMISTRY B

Article

pubs.acs.org/JPCB

The Presence of Ultralow Densities of Nanocrystallites in Amorphous Poly(lactic acid) Microspheres

Hilton B. de Aguiar, Alex G. F. de Beer, and Sylvie Roke*

Laboratory for Fundamental Biophotonics (LBP), Institute of Bioengineering (IBI), School of Engineering (STI), École Polytechnique Fédérale de Lausanne (EPFL), 1015 Lausanne, Switzerland

ABSTRACT: Ultralow densities of crystalline nanospheres have been detected in amorphous polymer microspheres by utilizing the unique sensitivity of second-order nonlinear optical techniques to anisotropy. Vibrational sum frequency scattering (SFS) and X-ray diffraction (XRD) are used to quantify the crystallinity of amorphous poly(D,L-lactic acid) microspheres. While XRD does not display any crystallinity for the microspheres, SFS spectra and patterns are reminiscent of a heterogeneous microsphere that contains small crystalline domains. Nonlinear light scattering theory was used to model the data, and an average domain radius of 147 ± 65 nm was obtained. The degree of crystallinity (0.2%) was estimated by comparing XRD and SFS data obtained from the amorphous microspheres to similar data obtained from crystalline microspheres. We estimate a detection limit of 0.002% for SFS.

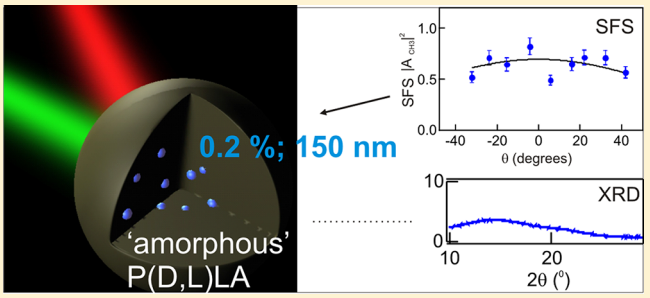

Crystallinity plays an important role in biology, chemistry, and physics. The structural, mechanical, and chemical properties of materials are strongly influenced by trace amounts of nanocrystallites. Protein crystallization is often the first step toward structure determination, and many pharmaceutical compounds depend on materials that have subtle changes in the degree of crystallinity. An example of a medicinal compound is the use of poly(lactic acid) (PLA) microspheres that have an embedded radio-activated Holmium complex. These microspheres are being pursued as future candidates for treating secondary liver cancer.[1,2]

PLA as a matrix material is extremely useful, as it is biodegradable and exists in many forms. PLA with a high degree of crystallinity can be made using only L-lactic acid (PLLA) or only D-lactic acid (PDLA) monomers. If both enantiomers are used as monomers, the material displays a low degree of crystallinity. A 50/50 mixture of D- and L-lactic acid monomers (P(D,L)LA) displays no detectable crystallinity.[3] The degree of crystallinity (X_c) is defined as the ratio of crystalline material to the total material (crystalline plus amorphous) and can be determined by X-ray diffraction (XRD)[4] or thermal measurements.[3,5] A comparison of XRD data of amorphous and crystalline PLA is shown in Figure 1.

Second-order nonlinear optical techniques, such as second-harmonic generation (SHG) and sum frequency generation (SFG), can be used to probe anisotropy in materials because the second-order susceptibility ($\chi^{(2)}$) that is probed vanishes in centrosymmetric materials. As a consequence, the generation of second-harmonic, difference frequency, or sum frequency light can be used for optical parametric generation processes. The processes can also be used to measure chemical structure at interfaces.[6−9] Another application is the fast and sensitive detection of chiral molecules[10,11] and crystallites.[12−15] Second-harmonic[16] and sum frequency[17] scattering[18] are combinations of SHG and SFG with light scattering that can be useful to probe the surface[17,19] or the bulk[20] of particles in a solid or liquid matrix. Detection of the scattering pattern and the angle-resolved coherent vibrational spectrum can provide information about the molecular structure and the size and shape of particles.[20]

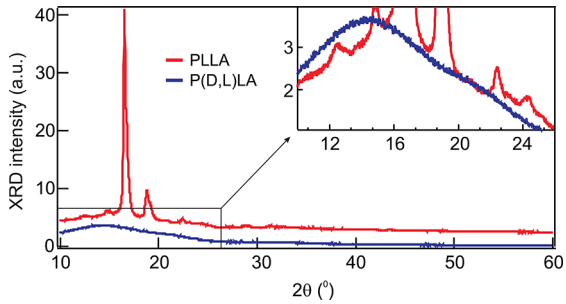

Figure 1. XRD data of PLLA and P(D,L)LA microspheres (offset for clarity). The presence of diffraction peaks for the PLLA microspheres classifies them as being composed of a semicrystalline polymer. The inset shows a magnified region of the XRD pattern in which no peak is observed for the P(D,L)LA microspheres.

Sum frequency generation studies of the interface of PLA films[21] have shown that the degree of surface (and bulk) ordering in PLAs can be tracked very well. Crystalline PLLA films display spectroscopic signatures reminiscent of ordered bulk and surface domains, whereas racemic P(D,L)LA films

Received: April 8, 2013
Revised: July 1, 2013
Published: July 2, 2013

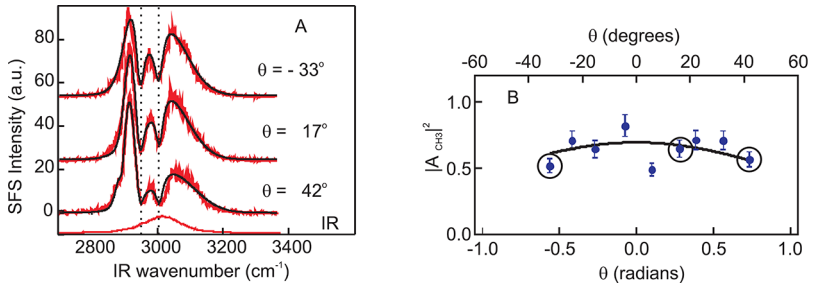

Figure 2. (A) SFS spectra of P(D,L)LA microspheres at different scattering angles (θ). Black lines are fits to eq 1. The lower spectrum is a profile of the IR pulse. The spectra are offset for clarity. (B) Normalized SFS pattern of the symmetric CH_3 stretching (2942 cm^{-1}) as retrieved from fits to the spectra. The black line is a fit to eq 2 from which we retrieve the size of the crystalline domains in the P(D,L)LA microspheres (R = 147 nm).

display hardly any organization on their surfaces. Semicrystalline PLLA microspheres were shown to consist of crystalline domains with a mean radius of 565 nm embedded in amorphous material.[20]

Here, we further explore the use of vibrational sum frequency scattering (SFS) to probe trace amounts of nanocrystallites in microspheres made of racemic poly(lactic acid). Racemic P(D,L)LA microspheres do not generate a signature of crystallinity in the X-ray diffraction pattern. They do, however, generate a sum frequency scattering pattern that is reminiscent of scattering by nanoscopic 147 nm domains. By comparison of SFS data from PLLA microspheres with a known degree of crystallinity to those of P(D,L)LA microspheres, the degree of crystallinity of P(D,L)LA micropsheres can be estimated. The found degree of crystallintiy is 0.2%, which shows that the amorphous racemic P(D,L)LA microspheres do have a small degree of order.

SFS BACKGROUND

In a typical SFS experiment, mid-infrared (ω_{IR}, IR) and visible (ω_{VIS}, VIS) laser pulses overlap in a dispersion and induce a second-order nonlinear polarization in the material. The polarization acts as a source for sum frequency (SF) photons with frequencies $\omega_{SFS} = \omega_{VIS} + \omega_{IR}$. Because of symmetry selection rules, the SFS process occurs only in noncentrosymmetric regions[22] (such as crystalline domains[20] and/or interfacial regions[17]). The generated SF photons emerge in an angular distribution that is determined by the nonlinear optical properties of the particle (contained in $\chi^{(2)}$), the size and shape of the particle, and the optical geometry (determined by the wavevectors $\mathbf{k}_{SF}$, $\mathbf{k}_{VIS}$, and $\mathbf{k}_{IR}$). The scattering angle θ is defined as the angle between the measured beam and the "phase-matched" forward direction $\mathbf{k}_{VIS} + \mathbf{k}_{IR}$.

Here, we are interested in the response of crystalline domains in SFS experiments. A description of the scattered spectra and the SF angular distribution originating from crystalline domains is given below (see ref 20 for more details). At a particular scattering angle θ, a spectrum is obtained that can be described by

$$I_{SFS}(\omega_{IR}, \theta) \propto \left| E_{IR}(\omega_{IR}) \left(A_{NR} e^{i\Delta\phi} + \sum_n \frac{A_n(\theta)}{(\omega_{IR} - \omega_{0n}) + i\Upsilon_n} \right) \otimes E_{VIS} \right|^2 \quad (1)$$

where E_{VIS} refers to the VIS electric field, E_{IR} to the IR electric field, A_{NR} to the nonresonant background with a relative phase $\Delta\phi$, and n to a vibrational mode with resonance frequency ω_{0n}, amplitude A_n, and half-width at half-maximum Υ_n. The symbol $\otimes$ represents a convolution in the frequency domain. The amplitudes of the vibrational resonances are obtained through eq 1.

The amplitudes $A_n(\theta)$ are the field amplitudes for the scattered electric field. For each resonance, the scattering pattern for spherical crystalline domains with radius R and $\chi^{(2)}$ components $\chi^{(2)}_{abc}$, $\chi^{(2)}_{bca}$, and $\chi^{(2)}_{cba}$ is given by

$$I_{u_0,u_1,u_2}(\theta) \propto N E_{u_1}^2 E_{u_2}^2 \frac{k_0^4}{r_0^2} |F(qR)|^2 \left[(c_1 + c_2 \cos(2\theta) + c_3 \sin(2\theta)) \left((\chi^{(2)}_{bca})^2 + (\chi^{(2)}_{cab})^2 \right) + (c_4 + c_5 \cos(2\theta) + c_6 \sin(2\theta)) \chi^{(2)}_{bca} \chi^{(2)}_{cab} \right] \quad (2)$$

where (a,b,c) represents the coordinate system of the unit cell for the $P2_12_12_1$ space group of poly(lactic acid) and N is the number of crystallites. u_0,u_1,u_2 represents polarization combinations of the in- and outgoing beams. $q = 2k_0 \sin(\theta/2)$ is the modulus of the scattering wavevector, R the radius of the crystalline domains, and $\chi^{(2)}_{eff}$ a combination of the second-order electrical susceptibility elements. c_1–c_6 are coefficients that depend on the scattering geometry. For the geometry used here and the *ssp* polarization combination, they are 4, 0, 0, 1.8, 0, and 0, respectively. Polarization combinations are given in the order SF, VIS, IR; *s* refers to vertical (out of plane) polarized light, *p* refers to horizontal (in plane) polarized light.

In general, as can be seen from eq 2, the SFS patterns of different polarization combinations contain information about the bulk morphology of the crystalline domains and also about the (nonlinear) optical properties.[20] In the polarization combination *ssp* (and *spp*, *pss*, *sps*, and *sss*), however, the $\chi^{(2)}$ elements weigh only the intensity of the pattern, not the shape. For these polarization combinations, the SFS pattern can be used to find the form factor $F(qR)$ to retrieve the domain size R, which is the only fitting parameter (q is known).[23] A form factor for a large object will be sharply peaked in the forward direction, whereas a form factor with a broad distribution corresponds to small objects (with respect to the probing wavelength). For the remaining polarization combinations, the scattering pattern also depends on the relative contribution of the different $\chi^{(2)}$ elements. Therefore, depending on the crystal symmetry, one can also separate the optical properties from the morphology of the crystalline domains.

RESULTS AND DISCUSSION

Powder X-ray diffraction (XRD) was used to characterize the crystallinity of partially crystalline PLLA and amorphous P(D,L)LA microspheres. The amplitude of the diffraction peaks in the XRD pattern reflects the extent of the crystalline

dx.doi.org/10.1021/jp4034497 | J. Phys. Chem. B 2013, 117, 8906–8910

domains within the microspheres. Figure 1 shows the XRD data of both PLLA and P(D,L)LA microsphere powder samples. The XRD pattern of PLLA shows the most prominent peaks at 2θ = 16.5° and 18.8° in accordance with previous studies.[24] The lack of diffraction peaks in the XRD pattern of P(D,L)LA microspheres shows that it consists of amorphous material, which is in agreement with differential scanning calorimetry (DSC) results.[3]

On the basis of the XRD results, it can be expected that the PLLA microspheres generate a strong scattering signal, whereas the amorphous P(D,L)LA microspheres do not. Figure 2A shows three representative SFS spectra of P(D,L)LA microspheres taken at different angles as well as a representation of the IR intensity envelope. The P(D,L)LA spectra display the shape of a broad, nearly Gaussian response that coincides with the IR pulse envelope. This nonresonant response interferes destructively with the two main spectral bands centered around ~2942 and ~3000 cm^{-1}. These two bands are the vibrational resonances of the symmetric and antisymmetric CH_3 stretches, respectively.[25] The solid lines shown in Figure 2A are fits to the data using eq 1 and resonances at 2889 cm^{-1} (C−H stretch, a minor contribution) and 2942 and 2998 cm^{-1} (the CH_3 symmetric and antisymmetric stretches, respectively).[21,26]

Figure 2B shows the intensity of the symmetric stretch mode as a function of scattering angle as retrieved from the fits to the spectra for a wide angular range. SFG originates from noncentrosymmetric regions. Here, this could be crystallites or interfaces (from either crystalline domains or the 20 μm microspheres). The scattering pattern does not vanish close to $\theta = 0°$ and is not sharply peaked. A vanishing signal at $\theta = 0°$ is characteristic of SFS that originates from a particle interface.[17,27] A sharply peaked scattering pattern would result from the microsphere−air interface. Indeed, any closed surface will have a scattering pattern that vanishes around $\theta = 0°$, so that even the assumption of spherical domains is not critical.[28] Quadrupolar bulk scattering will lead to a scattering pattern with the same characteristics.[29] Therefore, an interface cannot be the source of the scattering. As the interfacial response can be excluded, we can fit the SFS pattern of Figure 2B to eq 2 (black line). There is only one fit parameter, R, because the angular dependence is determined by only the form factor $F(qR)$. The radius for the best fit is found to be 147 ± 65 nm. Fitting our data with a straight line, which would point toward crystallites or ordered domains in the 1−10 nm range (comparable to structures probed with hyper-Rayleigh scattering), results in a chi-squared value that is 10% worse. It should be noted that a straight line is a possible outcome of the model and does not contradict the conclusions drawn.

Having determined the radius of the crystallites, we can estimate the degree of crystallinity by comparing the SF intensity of P(D,L)LA microspheres to that of PLLA microspheres that have a known degree of crystallinity. Figure 3 shows SFS spectra for PLLA and P(D,L)LA microspheres that were measured under identical conditions. It can be seen that the PLLA microspheres generate a much stronger SFS signal. Following refs 30 and 31, the relationship between the SFS intensity (I_{SFS}) and the domain radius (R) is given by

$$I_{SFS} \propto X_c R^3 \tag{3}$$

Therefore, the ratio of the degree of crystallinity of P(D,L)LA $X_{c,P(D,L)LA}$ to $X_{c,PLLA}$ is given by

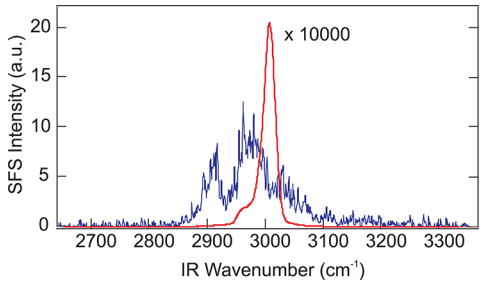

Figure 3. Comparison of the SFS spectra of PLLA (rescaled by a factor of 10^4) and P(D,L)LA microspheres. The measurement was performed at $\theta = 0°$, using the polarization combination *ssp*.

$$\frac{X_{c,P(D,L)LA}}{X_{c,PLLA}} = \frac{I_{P(D,L)LA}}{I_{PLLA}}\left(\frac{R_{PLLA}}{R_{P(D,L)LA}}\right)^3 \tag{4}$$

Using $X_{c,PLLA}$ = 0.35,[4] R_{PLLA} = 565 nm,[20] $R_{P(D,L)LA}$ = 147 nm, and $(I_{P(D,L)LA})/(I_{PLLA}) = 10^{-4}$ (Figure 3), we obtain $X_{c,P(D,L)LA}$ = 0.2%. For the limiting values of R = 147 ± 65 nm, we find $X_{c,P(D,L)LA}$ = 1.1% (R = 212 nm) and $X_{c,P(D,L)LA}$ = 0.07% (R = 82 nm), respectively. Because the detection limit of a standard XRD instrument is $X_c \approx 5\%$,[32] it is not surprising that the XRD results do not show any trace of crystallinity while the nonlinear light scattering measurements do show a small amount of crystallinity. The detection limit of SFS is ~100 times below the signals reported in this work. Given the same geometry and material, this leads to a limit of X_c = 0.002% for the detectable amount of trace crystallinity in solids (R = 147 nm). Thus, we find that P(D,L)LA polymer microspheres, which are generally considered to be amorphous, do have tiny traces of crystalline nanospheres. It is tempting to speculate that similar findings are true for other materials.

CONCLUSIONS

In summary, we have used the well-known sensitivity of second-order nonlinear optical techniques to anisotropic structures in combination with light scattering to probe the average nanocrystallite size and degree of crystallinity in amorphous poly(lactic acid) microspheres. From the vibrational sum frequency scattering experiments on poly(lactic acid) microspheres we found an average nanocrystalline domain size of 147 ± 65 nm and a total degree of crystallinity of 0.2%. This indicates that even in "completely amorphous" systems some ordering persists over a short length scale. Our work fits in the trend of using nonlinear optical methods to characterize biological systems, e.g., the use of SH microscopy to characterize protein crystals[33] and the use of SF microscopy[34] and SFG to analyze atmospheric particles.[35] It could also indicate that nanocrystallites may already be present in a wide range of amorphous systems and thus influence the physicochemical properties. Because small nanograins or cores can have large consequences for the mechanical and chemical properties of a material, the wider application of nonlinear optical methods for material characterization is a very useful one.

MATERIALS AND METHODS

The setup used for the SFS experiments was described elsewhere in detail.[36] IR pulses centered around 3000 cm^{-1} (6 μJ, 150 fs, fwhm bandwidth 120 cm^{-1}) were spatially and temporally overlapped with 800 nm VIS pulses (3 μJ, fwhm

dx.doi.org/10.1021/jp4034497 | J. Phys. Chem. B 2013, 117, 8906−8910

bandwidth 5 cm^{-1}). The angle between IR and VIS pulses was 15°, and the beams were focused down to a ≈0.4 mm beam waist. The scattered light was collimated with a lens, polarization selected, and spectrally dispersed onto an intensified CCD camera. The angular resolution was 10° set by the width of the slit placed in front of the collimating lens. All spectra shown were taken in the *ssp* polarization combination (*s*, sum frequency; *s*, visible; and *p*, IR) and divided by VIS and IR intensities and acquisition time.

The microspheres consisted of PLA polymers and had a broad size distribution of 10−25 μm in radius. Details of the preparation of the microspheres can be found elsewhere.[1] The (dried) microspheres were gently pressed between two CaF_2 windows, with a spacing of ≈100 μm, such that only a few microspheres were probed, thus minimizing multiple scattering effects.

AUTHOR INFORMATION

Corresponding Author

*E-mail: sylvie.roke@epfl.ch.

Notes

The authors declare no competing financial interest.

ACKNOWLEDGMENTS

We thank Udo Welzel for the XRD measurements and F. W. Nijsen and W. Bult for providing the P(D,L)LA and PLLA microspheres. This work is supported by the Julia Jacobi Foundation.

REFERENCES

(1) Nijsen, J.; van Steenbergen, M.; Kooijman, H.; Talsma, H.; Kroon-Batenburg, L.; van de Weert, M.; van Rijk, P.; de Witte, A.; van het Schip, A.; Hennink, W. Characterization of Poly(L-lactic acid) Microspheres Loaded with Holmium Acetylacetonate. *Biomaterials* **2001**, *22*, 3073−3081.

(2) Bult, W.; Vente, M. A. D.; Zonnenberg, B. A.; Van het Schip, A. D.; Nijsen, J. F. W. Microsphere Radioembolization of Liver Malignancies: Current Developments. *Quarterly Journal of Nuclear Medicine and Molecular Imaging* **2009**, *53*, 325−335.

(3) Tsuji, H.; Ikada, Y. Stereocomplex Formation between Enantiomeric Poly(lactic acid)s. 6. Binary Blends from Copolymers. *Macromolecules* **1992**, *25*, 5719−5723.

(4) Mano, J. F. Structural Evolution of the Amorphous Phase during Crystallization of Poly(L-lactic acid): A Synchrotron Wide-Angle X-ray Scattering Study. *J. Non-Cryst. Solids* **2007**, *353*, 2567−2572.

(5) Sarasua, J.-R.; Prud'homme, R. E.; Wisniewski, M.; Borgne, A. L.; Spassky, N. Crystallization and Melting Behavior of Polylactides. *Macromolecules* **1998**, *31*, 3895−3905.

(6) Eisenthal, K. B. Liquid Interfaces Probed by Second-Harmonic and Sum-Frequency Spectroscopy. *Chem. Rev.* **1996**, *96*, 1343−1360.

(7) Vidal, F.; Tadjeddine, A. Sum-Frequency Generation Spectroscopy of Interfaces. *Rep. Prog. Phys.* **2005**, *68*, 1095−1127.

(8) Miranda, P.; Pflumio, V.; Saijo, H.; Shen, Y. Chain−Chain Interaction between Surfactant Monolayers and Alkanes or Alcohols at Solid/Liquid Interfaces. *J. Am. Chem. Soc.* **1998**, *120*, 12092−12099.

(9) Roke, S. Nonlinear Optical Spectroscopy of Soft Matter Interfaces. *ChemPhysChem* **2009**, *10*, 1380−1388.

(10) Fu, L.; Liu, J.; Yan, E. C. Y. Chiral Sum Frequency Generation Spectroscopy for Characterizing Protein Secondary Structures at Interfaces. *J. Am. Chem. Soc.* **2011**, *133*, 8094−8097.

(11) Simpson, G. J. Molecular Origins of the Remarkable Chiral Sensitivity of Second-Order Nonlinear Optics. *ChemPhysChem* **2004**, *5*, 1301−1310.

(12) Hall, V.; Simpson, G. Direct Observation of Transient Ostwald Crystallization Ordering from Racemic Serine Solutions. *J. Am. Chem. Soc.* **2010**, *132*, 13598−13599.

(13) Wanapun, D.; Kestur, U.; Kissick, D.; Simpson, G.; Taylor, L. Selective Detection and Quantitation of Organic Molecule Crystallization by Second Harmonic Generation Microscopy. *Anal. Chem.* **2010**, *82*, 5425−5432.

(14) Wanapun, D.; Kestur, U.; Taylor, L.; Simpson, G. Single Particle Nonlinear Optical Imaging of Trace Crystallinity in an Organic Powder. *Anal. Chem.* **2011**, *83*, 4745−4751.

(15) Kissick, D. J.; Wanapun, D.; Simpson, G. J. Second-Order Nonlinear Optical Imaging of Chiral Crystals. *Annu. Rev. Anal. Chem.* **2011**, *4*, 419−437.

(16) Wang, H.; Yan, E. C. Y.; Borguet, E.; Eisenthal, K. B. Second Harmonic Generation from the Surface of Centrosymmetric Particles in Bulk Solution. *Chem. Phys. Lett.* **1996**, *259*, 15−20.

(17) Roke, S.; Roeterdink, W. G.; Wijnhoven, J. E.; Petukhov, A. V.; Kleyn, A. W.; Bonn, M. Vibrational Sum Frequency Scattering from a Submicron Suspension. *Phys. Rev. Lett.* **2003**, *91*, 258302.

(18) Eisenthal, K. B. Second Harmonic Spectroscopy of Aqueous Nano- and Microparticle Interfaces. *Chem. Rev.* **2006**, *106*, 1462−1477.

(19) de Aguiar, H. B.; de Beer, A. G. F.; Strader, M. L.; Roke, S. The Interfacial Tension of Nanoscopic Oil Droplets in Water Is Hardly Affected by SDS Surfactant. *J. Am. Chem. Soc.* **2010**, *132*, 2122−2123.

(20) de Beer, A. G. F.; de Aguiar, H. B.; Nijsen, J. F. W.; Sugiharto, A. B.; Roke, S. Detection of Buried Microstructures by Nonlinear Light Scattering Spectroscopy. *Phys. Rev. Lett.* **2009**, *102*, 095502.

(21) Johnson, C. M.; Sugiharto, A. B.; Roke, S. Surface and Bulk Structure of Poly-(lactic acid) Films Studied by Vibrational Sum Frequency Generation Spectroscopy. *Chem. Phys. Lett.* **2007**, *449*, 191−195.

(22) Boyd, R. W. *Nonlinear Optics*, 2nd ed.; Academic Press, 2003.

(23) Kerker, M. *Scattering of Light and Other Electromagnetic Radiation*; Academic Press, 1969.

(24) Brizzolara, D.; Cantow, H.-J.; Diederichs, K.; Keller, E.; Domb, A. J. Mechanism of the Stereocomplex Formation between Enantiomeric Poly(lactide)s. *Macromolecules* **1996**, *29*, 191−197.

(25) Lambert, A.; Davies, P. B.; Neivandt, D. J. Implementing the Theory of Sum Frequency Generation Vibrational Spectroscopy: A Tutorial Review. *Appl. Spectrosc. Rev.* **2005**, *40*, 103−145.

(26) Aou, K.; Hsu, S. L. Trichroic Vibrational Analysis on the α-Form of Poly(lactic acid) Crystals Using Highly Oriented Fibers and Spherulites. *Macromolecules* **2006**, *39*, 3337−3344.

(27) Shan, J.; Dadap, J. I.; Stiopkin, I.; Reider, G. A.; Heinz, T. F. Experimental Study of Optical Second-Harmonic Scattering from Spherical Nanoparticles. *Phys. Rev. A* **2006**, *73*, 023819.

(28) de Beer, A. G. F.; Roke, S.; Dadap, J. Theory of Optical Second-Harmonic and Sum-Frequency Scattering from Arbitrarily Shaped Particles. *J. Opt. Soc. Am. B* **2011**, *28*, 1374−1384.

(29) de Beer, A. G. F.; Roke, S. Nonlinear Mie Theory for Second-Harmonic and Sum-Frequency Scattering. *Phys. Rev. B* **2009**, *79*, 155420.

(30) de Aguiar, H. B.; Samson, J.; Roke, S. Probing Nanoscopic Droplet Interfaces in Aqueous Solution with Vibrational Sum-Frequency Scattering: A Study of the Effects of Path Length, Droplet Density and Pulse Energy. *Chem. Phys. Lett.* **2011**, *512*, 76−80.

(31) de Aguiar, H. B.; Scheu, R.; Jena, K. C.; de Beer, A. G. F.; Roke, S. Comparison of Scattering and Reflection SFG: A Question of Phase-Matching. *Phys. Chem. Chem. Phys.* **2012**, *14*, 6826−6832.

(32) Kitahara, S.; Ishizukaa, T.; Kikkojia, T.; Matsudab, R.; Hayashi, Y. Precision and Detection Limit of Quality Test for Amorphous Drug in Powder X-ray Diffractometry. *Int. J. Pharm.* **2004**, *283*, 63−69.

(33) Wampler, R. D.; Kissick, D. J.; Dehen, C. J.; Gualtieri, E. J.; Grey, J. L.; Wang, H. F.; Thompson, D. H.; Cheng, J. X.; Simpson, G. J. Selective Detection of Protein Crystals by Second Harmonic Microscopy. *J. Am. Chem. Soc.* **2008**, *130*, 14076−14077.

(34) Cai, X.; Hu, B.; Sun, T.; Kelly, K. F.; Baldelli, S. Sum Frequency Generation-Compressive Sensing Microscope. *J. Chem. Phys.* **2011**, *135*, 194202.

(35) Ebben, C. J.; Shrestha, M.; Martinez, I. S.; Corrigan, A. L.; Frossard, A. A.; Song, W. W.; Worton, D. R.; Petäjä, T.; Williams, J.;

Russell, L. M.; et al. Organic Constituents on the Surfaces of Aerosol Particles from Southern Finland, Amazonia, and California Studied by Vibrational Sum Frequency Generation. *J. Phys. Chem. A* **2012**, *116*, 8271−8290.

(36) Sugiharto, A. B.; Johnson, C. M.; De Aguiar, H. B.; Alloatti, L.; Roke, S. Generation and Application of High Power Femtosecond Pulses in the Vibrational Fingerprint Region. *Appl. Phys. B: Lasers Opt.* **2008**, *91*, 315−318.